

## Endogenous phosphotyrosine signaling in zebrafish embryos

Simone M. Lemeer<sup>1,2</sup>, Rob Ruijtenbeek<sup>3</sup>, Martijn W.H. Pinkse<sup>1</sup>, Chris Jopling<sup>2</sup>,  
Albert J.R. Heck<sup>1</sup>, Jeroen den Hertog<sup>2</sup>, and Monique Slijper<sup>1</sup>

<sup>1</sup> Department of Biomolecular Mass Spectrometry, Bijvoet Center for Biomolecular Research and Utrecht Institute for Pharmaceutical Sciences, Utrecht University, Sorbonnelaan 16, 3584 CA Utrecht, The Netherlands

<sup>2</sup> Netherlands Institute for Developmental Biology, Hubrecht Laboratory, Uppsalalaan 8, 3584 CT Utrecht, The Netherlands

<sup>3</sup> Pamgene International B.V., Nieuwstraat 30, 5211 BJ 's Hertogenbosch, The Netherlands

Corresponding authors,

Dr. M. Slijper: Tel: 31-30-2533789; Fax 31-30-2518219; E-mail: [m.slijper@uu.nl](mailto:m.slijper@uu.nl)

Dr. J. den Hertog: Tel.: 31-30-2121800; Fax: 31-30-2516464; E-mail: [hertog@niob.knaw.nl](mailto:hertog@niob.knaw.nl)

## Abstract

In the developing embryo, cell growth, differentiation and migration are strictly regulated by complex signaling pathways. One of the most important cell signaling mechanisms is protein phosphorylation on tyrosine residues, which is tightly controlled by protein-tyrosine kinases and protein-tyrosine phosphatases. Here, we investigated endogenous phosphotyrosine signaling in developing zebrafish embryos. Tyrosine phosphorylated proteins were immuno-affinity purified from zebrafish embryos at 3 and 5 days post fertilization and identified by multi-dimensional LC-MS. Amongst the identified proteins were tyrosine kinases, including Src family kinases, Eph receptor kinases and Focal adhesion kinases as well as the adaptor proteins, Paxillin, p130Cas and Crk. We identified several known and some unknown *in vivo* tyrosine phosphorylation sites in these proteins. Whereas most immuno-affinity purified proteins were detected at both developmental stages, significant differences in abundance and/or phosphorylation state were also observed. In addition, multiplex *in vitro* kinase assays were performed by incubating a micro-array of peptide substrates with the lysates of the two developmental stages. Many of the *in vivo* observations were confirmed by this on-chip *in vitro* kinase assay. Our experiments are the first to show that global tyrosine phosphorylation mediated signaling can be studied at endogenous levels in complex multicellular organisms.

## Introduction

Embryonic development is tightly regulated and numerous developmental processes like cell growth, differentiation and migration are controlled by phosphotyrosine signaling, which is mediated by protein-tyrosine kinases (PTKs) and protein-tyrosine phosphatases (PTPs). Improved knowledge about the identity of tyrosine phosphorylated proteins, their interacting proteins and their involvement in signaling will improve our understanding of biological pathways and critical cellular processes. A first step towards elucidation of the critical signaling pathways is the identification of tyrosine phosphorylated proteins in the developing embryo.

In recent years the availability of selective antibodies (1-4), targeted at tyrosine phosphorylated proteins, facilitated more global purification of these proteins and their binding partners, allowing identification by very sensitive LC MS-based analysis of the proteins tryptic digests (1,4,5). Such approaches have been used for instance to study elegantly the temporal, global response to receptor stimulation. However, all of these data have been obtained from well defined cell systems, under stimulated conditions. Although these data contribute well to our understanding of complex tyrosine phosphorylation mediated signaling pathways, it is still unclear how they relate to *in vivo* processes. Therefore, *in vivo* studies are essential (6). Here we explore whether the above described technologies may be extended to perform a global analysis of *in vivo* signaling processes involved in zebrafish development. Zebrafish is now an established model organism for vertebrate development and human disease (7,8). Zebrafish embryos are optically transparent, fertilization is external and after 5 days of development most organs are formed, making it an ideal system to study development. Indeed, by identifying mutations in key signaling molecules, direct insight into many signaling pathways involved in development was given (9,10). However a global

insight in the post-translational modifications at the complex level of the whole organism has not been obtained.

Here, we set out to evaluate whether the global analysis of endogenous tyrosine phosphorylation mediated signaling processes involved in zebrafish development is feasible by analysis of their proteomes at two different developmental stages, 3 and 5 days post fertilization (dpf). Embryogenesis of the zebrafish is a matter of days, and large numbers of zebrafish embryos can be obtained. A large amount of starting material is a prerequisite for proteomics studies and even more so for phosphoproteome analyses. Rigorous enrichment of tyrosine phosphorylated proteins is essential, because tyrosine phosphorylated proteins usually represent only 0.05% of the total amount of protein in a vertebrate cell (1,2,11). The analysis of a complex multi cellular organism forms an extra challenge compared to *in vitro* cell lines, comprising a single cell type. Therefore, we chose a number of enrichment steps, consisting of immunoprecipitation of tyrosine phosphorylated proteins by a mixture of antibodies. Following proteolysis of the enriched proteins, the peptides were first separated by strong cation exchange chromatography, where after the generated peptide fractions were further separated by reversed phase (RP) chromatography, followed by mass spectrometric detection using a LTQ-FT-ICR mass spectrometer. This approach led to the identification of 800 immunoprecipitated proteins or their co-immunoprecipitating interacting partners, not necessarily tyrosine phosphorylated themselves (5). In addition, we identified 16 tyrosine phosphorylation sites and 3 serine phosphorylation sites on 14 proteins. The obtained *in vivo* results were further validated by immunoblotting and *in vitro* kinase assays using peptide micro-array chips.

## Materials and Methods

### *Embryo Lysis and Immunoprecipitation*

Embryos were grown till 3 or 5 dpf. At 3 dpf, embryos were de-yolked with de-yolk buffer ( $\frac{1}{2}$  Ginzburg Fish Ringer) without calcium (12,13). Subsequently, embryos were lysed in buffer containing 50 mM Tris pH 7.5, 150 mM NaCl, 1 mM EDTA, 1 mM sodium orthovanadate, 1% NP-40, 0.1% sodium deoxycholate and protease inhibitor cocktail (Complete Mini, Roche Diagnostics, Almere, the Netherlands) and sonicated for 15 seconds. Lysates were centrifuged at 14,000 *g* to pellet cellular debris. Protein concentration was determined by a Quant Kit (Amersham Biosciences/GE healthcare, Uppsala, Sweden), using the standard protocol. For each experiment, 10-25 mg of protein was used (corresponding to 1000-2000 embryo equivalents) as starting material from both samples. Lysates were pre-cleared on protein A Sepharose beads (GE Healthcare, Diegem, Belgium) for 1 hr at 4 °C to reduce non-specific binding of abundant proteins. Protein A beads were separated from the lysate by centrifugation. PY20 antibody (BD Transduction Laboratories, Alphen a/d Rijn, the Netherlands) was incubated with each of the two lysates for 1 hr followed by the addition of protein A/G Plus beads (Santa Cruz Biotechnology, Heidelberg, Germany) for 1 hr. Finally, agarose-conjugated pTyr-100 (Cell Signaling Technology, Danvers, USA) was added for overnight incubation. Precipitated proteins and complexes were washed extensively with HNTG-Buffer (50 mM Hepes pH 7.4, 150 mM NaCl, 10% glycerol and 0.1 % Triton X-100). Bound proteins were eluted with 3 column volumes of 100 mM phenylphosphate (Sigma, Zwijndrecht, the Netherlands) in PBS at RT. The buffer was exchanged to ammonium bicarbonate (25 mM) pH 8.5 and samples were concentrated using a Millipore spin-column (5 kDa MW cutoff) (Millipore, Amsterdam, the Netherlands). Eluates were diluted in 8 M urea/25 mM ammonium bicarbonate and Lys-C (Roche Diagnostics) was added. Digestion was performed for 4 hrs at RT. Samples were reduced with DTT at a final concentration of 2

mM at 56 °C, subsequently samples were alkylated with iodoacetamide at a final concentration of 8 mM at RT. The eluate was diluted to 2 M Urea/50 mM ammoniumbicarbonate and trypsin (Roche Diagnostics) was added. Digestion was performed overnight at 37°C.

For Paxillin and EphA4 reversed immunoprecipitation experiments, lysates were prepared and precleared as described above. Paxillin (BD Transduction Laboratories) or EphA4 (kindly provided by Dr. D. Wilkinson, Division of Developmental Neurobiology, National Institute for Medical Research, The Ridgeway, Mill Hill, London, UK) antibody was incubated with each of the two lysates for 1 hr followed by the addition of protein A/G Plus beads for overnight incubation. Precipitated proteins were washed extensively with HNTG. Bound proteins were eluted by boiling the beads in 2x sample buffer for 5 min at 95°C.

#### *Immunoblotting*

For immunoblotting experiments, lysate and eluates from the immunoprecipitations were obtained as described above. Lysates (40 µg, corresponding to 5 embryo equivalents) and immunoprecipitates (corresponding to 75 embryo equivalents) were loaded on SDS-PAGE and blotted. After transfer the membrane was stained with Coomassie Blue Stain to verify equilading of the lysates. Subsequently the PVDF membrane was blocked with 2% BSA and then incubated with the corresponding antibodies against phosphotyrosine (PY20), pSrc418 (both from BioSource Technologies), Actin (Sigma), EphA4 and Paxillin, followed by the HRP-conjugated secondary antibody. The membranes were subjected to detection by enhanced chemiluminescence.

### *SCX chromatography*

Strong cation exchange was performed using a Zorbax BioSCX-Series II columns (ID: 0.8 mm x 1: 50 mm, particle size: 3.5  $\mu\text{m}$ ), a Famos autosampler (LCpackings, Amsterdam, The Netherlands), a Shimadzu LC-9A binary pump and a SPD-6A UV-detector (Shimadzu, Tokyo, Japan). Prior to SCX chromatography, protein digests were desalted using a small plug of C18 material (3M Empore C18 extraction disk) packed into a GELoader Tip as previously described (14). The eluate was dried completely by vacuum centrifugation and subsequently reconstituted in 20% acetonitrile, 0.05% formic acid. After injection, the first 10 minutes were run isocratically at 100% solvent A (0.05% formic acid in 8/2 (v/v) water/acetonitrile, pH 3.0), followed by a linear gradient of 1.3%  $\text{min}^{-1}$  solvent B (500 mM NaCl in 0.05% formic acid in 8/2 (v/v) water/acetonitrile, pH 3.0). A total number of 25 SCX fractions (1 min each, *i.e.* 50  $\mu\text{L}$  elution volume) were manually collected and dried in a vacuum centrifuge.

### *On-line nanoflow liquid chromatography FT-ICR-MS.*

Nanoflow LC-MS/MS was performed by coupling an Agilent 1100 HPLC system (Agilent Technologies, Waldbronn, Germany) to a 7-Tesla LTQ-FT-ICR mass spectrometer (Thermo Electron, Bremen, Germany) as described previously (15). Dried fractions were reconstituted in 10  $\mu\text{L}$  0.1 M acetic acid and delivered to a trap column (Aqua<sup>tm</sup> C18, 5  $\mu\text{m}$ , Phenomenex, Torrance, CA, USA); 20 mm  $\times$  100  $\mu\text{m}$  ID, packed in-house) at 5  $\mu\text{L}/\text{min}$  in 100% solvent A (0.1 M acetic acid in water). Subsequently peptides were transferred to an analytical column (ReproSil-Pur C18-AQ, 3  $\mu\text{m}$ , Dr. Maisch GmbH, Ammerbuch, Germany; 25cm  $\times$  50  $\mu\text{m}$  ID, packed in-house) at  $\sim$ 150 nL/min in a 50-min gradient from 0 to 40% solvent B (0.1 M acetic acid in 8/2 (v/v) acetonitrile/water). The eluent was sprayed via emitter tips (made in-house), butt-connected to the analytical column. The mass spectrometer

was operated in data dependent mode, automatically switching between MS and MS<sup>2</sup> and neutral loss driven MS<sup>3</sup> acquisition. Full scan MS spectra (from  $m/z$  300-1500) were acquired in the FT-ICR with a resolution of 100,000 at  $m/z$  400 after accumulation to target value of 500,000. The three most intense ions at a threshold above 5000 were selected for collision-induced fragmentation in the linear ion trap at normalized collision energy of 35% after accumulation to a target value of 15,000. The data-dependent neutral loss settings were chosen to trigger an MS<sup>3</sup> event after a neutral loss of either 24.5, 32.6 or  $49 \pm 0.5$   $m/z$  was detected amongst the 5 most intense fragment ions, to determine serine and threonine phosphorylation.

#### *Data analysis*

All MS<sup>2</sup> and MS<sup>3</sup> spectra were converted to single DTA files using Bioworks 3.1. An in-house developed Perl script was used to assign for each MS<sup>3</sup> spectrum the original and accurate parent mass from the full scan, enabling an accurate mass search for these spectra as well. Eventually, all MS<sup>2</sup> and MS<sup>3</sup> spectra from each LC-MS run were merged to a single file, which was searched using the Mascot search engine (Matrix Science, London, UK, version 2.1.02) against the IPI zebrafish database (version 3.16; 46700 entries) with carbamidomethyl cysteine as fixed modification. Protein N-acetylation, methionine oxidation, and phosphorylation of serine, threonine or tyrosine were specified as variable modifications. Trypsin was specified as the proteolytic enzyme and up to two missed cleavages were allowed. The mass tolerance of the precursor ion was set to 15 ppm and that of fragment ions was set to 0.9 Da. All phosphorylated peptides identified during Mascot searches were confirmed by manual interpretation of the spectra. Scaffold (version Scaffold-01\_05\_00, Proteome Software Inc., Portland, OR, USA) was used to validate MS<sup>2</sup> based peptide and protein identifications. Peptide identifications were accepted if they could be established at



greater than 95.0% probability as specified by the Peptide Prophet algorithm (16). Protein identifications were accepted if they could be established at greater than 99.0% probability and contained at least 2 identified peptides. Protein probabilities were assigned by the Protein Prophet algorithm (16). A BLAST tool (<http://www.ncbi.nlm.nih.gov/blast/>) was used to identify protein names from their sequence. IPI zebrafish proteins annotated as 'unknown' or 'hypothetical' were searched for regions of local similarity between sequences in the NCBI-nr database, using a BLAST search engine, to extract supplementary information about this protein, such as putative function and protein family. For this an in-house Perl script was developed that extracts the IPI zebrafish protein sequences from a FASTA database followed by an automated blast search against NCBI-nr. Chosen settings for BLAST (NCBI version 2.2.11) with an e-value cutoff off  $1*10^{-4}$  and Blosum62, thus only proteins with a reasonable homology were retrieved and stored in a results file. Subsequently matches with an e-value between  $1*10^{-100}$  and  $1*10^{-200}$  (0.0) were regarded as close homologs (paralogs and orthologs cannot be ruled out with this method). Matches with higher e-values were used to deduce functional information or characteristics about the protein family.

#### *In vitro kinase assay*

Micro-array experiments were performed in triplicate using PamChip arrays (PamGene, 's Hertogenbosch, The Netherlands) run on a PamStation4 instrument (PamGene). This integrated micro-array platform allows automated running of samples including incubation by pumping the sample up and down through the 3-dimensional porous chip. The automated run includes data capturing by real-time imaging (fluorescence signal development is read-out by CCD imaging) and washing (17-20). A PamChip consists of four identical peptide micro-arrays, which run 4 samples in parallel during an experiment. The array used in this experiments comprised 144 different peptide (20). Each peptide represents a 15 amino

acid sequence, of which 13 residues are derived from a putative endogenous phosphorylation site. The used peptide sequences were derived from Swissprot and/or Phosphobase databases and are provided in the supplementary Table 2. Two N-terminal residues complete part of a spacer linking the phosphosite sequence to the solid support of the 3-dimensional chip.

3 and 5 dpf embryos were lysed in buffer containing 50 mM Tris pH 7.5, 150 mM NaCl, 1 mM sodium orthovanadate, 1% NP-40, 0.1% sodium deoxycholate and EDTA-free protease inhibitor cocktail (Sigma). Kinase activities in these lysates were analyzed in triplicate by applying 2.5-5 µg of total protein in 25 µl kinase reaction buffer (Abl reaction buffer from New England Biolabs (Westburg, Leusden, the Netherlands), consisting of 100 mM MgCl<sub>2</sub>, 10 mM EGTA, 20 mM DTT and 0.1 % Brij 35 in 500 mM Tris/HCl, pH 7.5). Additionally the kinase reaction buffer contained 12.5 µg/ml fluoresceine labeled PY20 antibody against phosphotyrosine (Exalpha, USA), and 400 µM ATP (Sigma) to the PamChip peptide microarray. As control, kinase reaction buffer without ATP was used to detect background signal intensity. Prior to application of the sample, the chips were blocked using a solution of 2% BSA in water (Bovine Serum Albumin, Fraction V, Calbiochem, Germany), and washed 2 times with kinase reaction buffer. During 60 minutes incubation at 30°C, real time images are taken automatically every other 3 minutes. Images were analyzed by BioNavigator software (PamGene, The Netherlands).

## Results

### *Identification of endogenous tyrosine phosphorylated proteins and their binding proteins in developing zebrafish embryos*

We set out to identify tyrosine phosphorylated proteins in zebrafish embryos at 3 and 5 dpf. Illustrative pictures of zebrafish at 3 and 5 dpf are shown in Fig. 1A. A scheme of the experimental set-up is provided in Fig. 1B: approximately 1500 embryos were lysed per experiment per time-point. Phosphotyrosine containing proteins were immunoprecipitated from these lysates using a mixture of anti-phosphotyrosine antibodies (PY20, pTyr-100). Elution specificity of the bound proteins in this preparative set-up was achieved by using phenylphosphate. Immunoprecipitation efficiency was evaluated by immunoblotting using anti-phosphotyrosine antibody (PY20), as depicted in Fig. 2. The anti-pTyr immunoblots shown in Fig. 2 reveal a clear enrichment of tyrosine phosphorylated proteins in the immunoprecipitated fractions for both 3 dpf and 5 dpf zebrafish (Fig. 2, lysate *versus* IP panel). Phenylphosphate elution was efficient as no tyrosine phosphorylated proteins were detected on the beads after elution (Fig. 2, beads panel). Reproducibly, higher phosphotyrosine signals and different protein patterns were detected on the immunoblots of the 3 and 5 dpf embryos, whereas lysates were loaded equally as verified by Coomassie staining of the immunoblot (data not shown).

Immunoprecipitated proteins from both stages were in-solution digested and the resulting peptide mixture was analyzed by SCX-RP-LC-MS/MS. This multi-dimensional LC approach has the advantage that the separation of complex peptide mixture is improved, allowing a more comprehensive analysis of all immunopurified proteins. In addition, SCX chromatography is known to enable targeted identification of phosphopeptides, since most of these peptides elute simultaneously in the early fractions (21). In total we cumulatively identified over 800 proteins using the zebrafish IPI database, as summarized in the

Supplementary Table 1 and comprehensively described in the supplementary Scaffold file (at [https://bioinformatics.chem.uu.nl/supplementary/lemeer\\_mcp](https://bioinformatics.chem.uu.nl/supplementary/lemeer_mcp)) . The zebrafish IPI database is not yet very well annotated, as many proteins were annotated as ‘unknown’ or ‘hypothetical’. To obtain an improved view of the potential function of these proteins, the functional annotations of many of the proteins were elucidated using BLAST searches and sequence alignments. We identified a large set of tyrosine kinases, which are expected to be phosphorylated on tyrosine (Table 1). In addition, we identified adaptor proteins that may be phosphorylated on tyrosine themselves or that co-immunoprecipitate with tyrosine phosphorylated proteins (Table 1). We used relatively mild lysis conditions that do not disrupt protein complexes and therefore allowed identification of co-immunoprecipitating proteins. Among the 800 identified proteins a large number of proteins were annotated as yolk, ribosomal, cytoskeleton, histone and other highly abundant “house-keeping” proteins. It is well known that a targeted pull-down approach for tyrosine phosphorylated proteins can be hampered by the concomitant pull-down of highly abundant proteins.

We focused on the large set of tyrosine kinases and associated signaling proteins. In Table 1 we list for these proteins the sequence coverage obtained by mass spectrometry and the number of cumulative unique peptides over 3 replicates. Whereas these numbers can not be taken as an absolute measure of their abundance in the immunoprecipitate, significant differences were observed between the immunoprecipitates of 3 dpf and 5 dpf. We note that many Eph receptor kinases are easier detected at 5 dpf than at 3 dpf. The adaptor protein paxillin seems to be easier to detect in the immunoprecipitate of 3 dpf when compared to 5 dpf (see Table 1). The sequence coverage we obtained for most tyrosine kinases and their adapter proteins remained mostly below 10%. Still, we were able to detect 19 phosphorylation sites derived from 14 proteins in both stages, whereby most of these were tyrosine phosphorylated sites. Four typical MS<sup>2</sup> spectra from the identified phosphopeptides are shown

in Fig. 3; a summary of all phosphopeptide MS<sup>2</sup> and MS<sup>3</sup> spectra is given in the supplementary data (Supplementary Spectra S1, S2). Identified phosphorylation sites from both samples were manually confirmed and are shown in Table 2, including their MASCOT score. The total number of tyrosine phosphorylation sites identified is not as high as in recently reported studies (1,4,5), due to the fact that all these earlier studies were on stimulated cells with relatively high phosphotyrosine levels, compared to the endogenous levels in the whole organism as studied here.

We identified several components of focal adhesions at 3 and 5 dpf, including Focal adhesion kinase (Fak) 1a and 1b. The Fak peptide YMEDSSYYK was shown to be phosphorylated on Tyr-7 or Tyr-8 (corresponding to Tyr-576 or Tyr-577 in human) in both the 3 and 5 dpf immunoprecipitates (Table 1, 2). The doubly phosphorylated peptide was only detected in the 5 dpf sample. Two well known substrates of Fak, paxillin and p130Cas, were also detected, but only in the 3 dpf immunoprecipitate. In paxillin we identified QGVFLPEETPpYSCPR, corresponding to Tyr-31 in human (Fig. 3A, Table 2) and thus a conserved tyrosine phosphorylation site from zebrafish to human. In p130Cas we identified 4 phosphopeptides, 2 tyrosine phosphorylated, one serine phosphorylated and one doubly phosphorylated (2 Ser) (Table 1, 2). None of the identified phosphopeptides from p130Cas have been previously reported, although for 3 of these sites (GPPSGQEIpYDTPPSVDK, RQPEGQEIpYDIPASLR, and RLpSASSTGSTR) partial sequence homology exists in human p130Cas (22,23).

Three members of the Src family of kinases, Fyn, Yes, and Src, were identified at both stages. Although these proteins have a high sequence homology we were able to identify at least 1 unique peptide for each protein at both stages, indicating that Fyn, Yes and Src are all three immunoprecipitated (Table 1). The total number of unique identified peptides in 3 replicates for the three Src family kinase members (Src, Fyn, Yes) together, is also given in

Table 1. The phosphopeptide LIEDNEpYTAR (autophosphorylation site Tyr-416 in human) was identified in 3 and 5 dpf embryos (Fig. 3B, Table 1, 2).

Another quite abundant family of tyrosine kinases identified in our screen is the Eph family of receptor tyrosine kinases. We detected peptides of many of the known Eph receptors both in the 3dpf and 5 dpf immunoprecipitates (Table 1). In the 5 dpf immunoprecipitate we also identified 4 phosphorylation sites on 4 different Eph receptors (Table 2, Fig. 3C).

The adaptor molecule Crk was identified in both the 3 and 5 dpf immunoprecipitate samples (Table 1). In the 5 dpf sample we were also able to identify a previously not reported serine phosphorylated peptide, LLDQHNPEDeLpS (Table 2). Mapk14a and Mapk14b were identified in the 3 and 5 dpf sample, including a phosphorylated site, that has been previously reported for the human homologue (Table 1, 2, Fig. 3D). Mapk12 was detected only in the 5 dpf sample, including a phosphorylated peptide (Table 1,2).

#### *In vitro tyrosine kinase activities in zebrafish embryos*

Concomitant with our *in vivo* screen for endogenous tyrosine phosphorylated proteins in zebrafish development, we performed an *in vitro* kinase assay using a peptide array (Fig. 4). Each micro-array contained 144 peptides originating from putative tyrosine phosphorylation sites in known proteins. Peptides on the chip are primarily derived from human protein sequences, but 9 phosphopeptides identified in our *in vivo* screen were present on the chip with likely sufficient sequence homology (Table 2, indicated in bold, Fig. 4D). A list of all peptides present on the chip can be found in supplementary Table 2. For our *in vitro* kinase assay we used lysates from 3 dpf and 5 dpf zebrafish, and performed the experiments in triplicate. These lysates were individually incubated on the peptide substrate chip in the presence of ATP. A fluorescently labeled anti-pTyr antibody (PY20) was used to monitor tyrosine phosphorylation of the peptide substrates. Typical endpoint images are shown in Fig.

4 (A-C). All the peptide substrates identified by mass spectrometry that were found to be phosphorylated *in vivo* were phosphorylated *in vitro* both after incubation with 3 dpf and 5 dpf lysates (Fig. 4A, B). Especially peptides derived from paxillin, EphA2, EphB3 and the Src family kinases demonstrated a high *in vitro* phosphorylation signal. In the negative control (Fig. 4C), without ATP, no phosphorylation was detected, revealing that the signals in Fig. 4A and B were generated by kinase activity present in the lysates. The relative signal of *in vitro* peptide phosphorylation was corrected for background and the 5 dpf spot intensities were plotted against the intensities from the 3 dpf spots (Fig. 4E). Spot intensities from both stages did not show significant differences, indicating similar kinase activities in both 3 and 5 dpf lysates.

In summary, the detection of protein tyrosine phosphorylation at 3 and 5 dpf by mass spectrometry is confirmed by the results of this *in vitro* phosphorylation assay, showing that indeed concomitant kinase activities are present, thus revealing the complementarities of these two methods.

#### *Validation of protein tyrosine phosphorylation by immunoblotting*

To further validate the *in vivo* mass spectrometry results, we used immunoblotting. Anti-pTyr immunoprecipitates were blotted and probed with antibodies specific for proteins identified by mass spectrometry, notably paxillin, Src and Eph receptor, with actin as control (Fig. 5). The blot probed with the paxillin antibody showed a decreased signal in the 5 dpf lysate compared to the 3 dpf lysate. A clear paxillin signal was observed in the 3 dpf eluate from the immunoprecipitation, but not in the 5 dpf immunoprecipitate (Fig. 5A), which is in line with the fact that we detected paxillin with more unique peptides and higher sequence coverage at 3 dpf than at 5 dpf (Table 1). The pSrc418 antibody gave a clear signal in the 3 dpf and 5 dpf lysates and in the immunoprecipitates, showing tyrosine phosphorylation. There

was however a significant shift in the 1D gel, both in the lysates and the immunoprecipitate (see Fig. 5B). This shift may result from cross reactivity with other Src family kinase members (Fig. 5B). The EphA4 antibody gave a signal in both the 3 dpf and 5 dpf lysates, showing higher intensity for the 3 dpf sample (Fig. 5C). This was also reflected in the immunoprecipitates of the 3 and 5 dpf samples. A slight shift in mass is observed in the immunoprecipitates, indicative for phosphorylation, although the signals are low. The actin antibody, which was used as control, gave equal signals in the lysates from both 3 and 5 dpf embryos, indicating equal loading.

We performed reverse immunoprecipitation experiments to corroborate tyrosine phosphorylation on paxillin and EphA4 (Fig. 5E and 5F, respectively). Anti-paxillin immunoprecipitates were blotted and probed with paxillin and subsequently with phosphotyrosine (PY20) antibody. Figure 5E shows that paxillin is indeed immunoprecipitated from the 3 dpf lysate. The amount of paxillin in the 5 dpf immunoprecipitate is much lower, which is in line with the paxillin expression profile in the lysates (Fig. 5A). After reprobing the blot with phosphotyrosine antibody we could only detect a tyrosine phosphorylation of paxillin in the 3 dpf sample, but not in the 5 dpf sample, showing that paxillin is indeed phosphorylated in 3 dpf embryos.

The EphA4 immunoprecipitates were first probed with EphA4 antibody. EphA4 is readily immunoprecipitated from both 3 and 5 dpf lysates (Fig. 5F). The EphA4 signal is however higher in the 3 dpf immunoprecipitate (Fig. 5F). After reprobing the blot with phosphotyrosine antibody we could detect a faint band in the 3dpf immunoprecipitate that shows a mass shift compared to the EphA4 immunoblot, indicative for its phosphorylation.



## Discussion

Here, we examined tyrosine phosphorylation mediated signaling during zebrafish development *in vivo* by mass spectrometry based proteomics and complementary *in vitro* using kinase assays with peptide substrate micro-arrays arrays. We performed our analyses on zebrafish embryos at 3 and 5 days post fertilization. The protein tyrosine phosphorylated sub-proteome was targeted in our analyses using anti phosphotyrosine-affinity purification (1,4,5). It is known that enrichment is essential, otherwise tyrosine-phosphorylated proteins are present at undetectable levels (24). We explored successfully whether these well-described methods can also be adopted to investigate tyrosine phosphorylation mediated signaling in whole vertebrate organisms, under natural, i.e. non-stimulated, conditions. Notably, when there is no artificial stimulation as in the *in vivo* experiment described here, tyrosine phosphorylation is under strict regulation of protein-tyrosine kinases and protein-tyrosine phosphatases, resulting in extremely low endogenous levels of tyrosine phosphorylated proteins. Additionally, by the nature of our experiments, localized tyrosine phosphorylation events in the whole organism become 'diluted' compared to *in vitro* experiments using single cell types. For the large scale analyses of tyrosine phosphorylation, mostly cultures of single cell types are taken, comprising typically  $10^8$ - $10^9$  cells per experiment (5,24,25) In our experiment we took 1000-2000 embryo equivalents, which contain a heterogenous cell population. Still, with our approach, we detected 16 interesting tyrosine phosphorylation sites. This compares very well with, for example, recent results with analyses on cultured cells that overexpress ErbB2, where 8 tyrosine phosphorylation sites were detected after treatment with Herceptin (24).

Immunoblot analysis showed that our immunoprecipitation approach was successful; a clear enrichment of tyrosine phosphorylated proteins was observed for both stages (Fig. 2). Although protein tyrosine phosphorylation seems to be reproducibly higher in the 3 dpf

embryos, this observation is not supported by a higher amount of tyrosine phosphorylated proteins or phosphopeptides detected in our MS analysis. It should be noted that 3 dpf embryos still contain a higher proportion of yolk proteins. Despite removal of the yolk, many yolk proteins, predominantly vitellogenins, are still present in proteomic profiles of early zebrafish embryos (26). These vitellogenins are notoriously sticky proteins which may bind to the antibody and interfere with anti-pTyr immunoprecipitation and immunoblotting.

Using extensive peptide separation methodologies, with SCX and nanoRP coupled to LTQ-FT-ICR-MS/MS we identified over 800 proteins in the immunoprecipitate, containing a smaller interesting sub-set of tyrosine kinases and adaptors/substrates that are likely to play a major role in developmental processes. Moreover, on these interesting proteins we were able to identify 19 phosphorylation sites of which several were not reported previously.

We focus our discussion on several of these more interesting tyrosine kinases and their substrate/adaptor proteins.

### *Focal Adhesion Signalling*

Focal adhesion proteins form a link between the extracellular matrix and the actin cytoskeleton. They play an important role in the transduction of adhesion and growth factor signals. Mouse embryos deficient in focal adhesion kinase (Fak) or paxillin die early, illustrating the importance of focal adhesions in development (10,27). Fak is a non-receptor tyrosine kinase that, in association with Src, phosphorylates paxillin at Tyr-31 (28). Zebrafish have two Fak genes, *fak1a* and *fak1b* that are both expressed during early development. Tyrosine phosphorylation of Tyr-576/Tyr-577, which is important for catalytic activation has also been observed in early developmental stages in zebrafish (29). We identified Fak1a and Fak1b in both 3 and 5 dpf samples. Tyrosine phosphorylation at Tyr-567 and Tyr-577 was

detected in our proteomics screen and could be confirmed by the *in vitro* kinase assay (Fig. 4A, B).

Paxillin, another major constituent of focal adhesions binds many proteins that are involved in changing the actin cytoskeleton, necessary for cell motility events associated with development. Paxillin has been described as one of the major tyrosine phosphorylated proteins in embryonic development (30). In our proteomics screen paxillin was identified in the 3 dpf embryo, with 8 cumulative unique peptides, while it was not detected in the immunoprecipitate of the 5 dpf sample. Furthermore, we identified the *in vivo* tyrosine phosphorylation of Tyr-31 (Table 1,2, Fig. 3A) in the 3 dpf embryo, a site that is known to become phosphorylated in response to cell adhesion (28).

Immunoblot analysis with a paxillin antibody validated that phosphorylated paxillin is immunoprecipitated from the 3dpf lysates and showed that expression is reduced in 5 dpf embryos compared to 3 dpf (Fig. 5A). In the reverse immunoprecipitation experiment, it was shown that paxillin could be immunoprecipitated from the 3 dpf lysates, but not from the 5 dpf lysates. Reprobing the blot with phosphotyrosine antibody clearly shows phosphorylation of paxillin in the 3 dpf immunoprecipitate, whereas no phosphorylated paxillin could be detected in the 5 dpf immunoprecipitate (Fig. 5E). *In vitro* kinase assay experiments also confirmed tyrosine phosphorylation of paxillin at Tyr-31 (Fig. 4A, B). However the paxillin Tyr-31 containing peptide was phosphorylated by both the 3 and 5 dpf lysates. Focal adhesion kinase is still active in 5 dpf embryos, and therefore the paxillin Tyr-31 peptide (which is present in equal amounts on all chips) is also phosphorylated *in vitro*. *In vivo* however, paxillin expression is reduced in 5 dpf embryos; suggesting that signaling of paxillin is regulated by expression levels rather than by phosphorylation. Together, three independent methods confirm tyrosine phosphorylation of paxillin in 3 dpf embryos. Interestingly,

phosphorylation of Tyr-31 of paxillin creates an SH2 binding site for Crk (28,31), a protein that was identified in our screen both in the 3 and 5 dpf samples.

In addition to Fak transphosphorylation and paxillin phosphorylation, recruitment of Src into the signaling complex also facilitates phosphorylation of p130Cas, which is a docking protein with well characterized roles in cell migration and invasion. Tyrosine phosphorylation of p130Cas is required for its binding to Crk, which induces signaling cascades leading to cell migration and extension (32). p130Cas was identified in the 3 dpf immunoprecipitate with 21 cumulative unique peptides, including some with detected phosphorylation sites. It was however only detected with 2 cumulative unique peptides in the 5 dpf sample (Table 1,2), suggesting down regulation. Expression differences of p130Cas could not be validated by immunoblot analysis since there is no zebrafish-specific antibody available. Together our results implicate that focal adhesion signaling is clearly dynamic from day 3 to day 5 in zebrafish embryogenesis.

#### *Src family kinases*

The Src family kinases, Src, Fyn and Yes, were detected in both immunoprecipitates, indicating that they likely are ubiquitously phosphorylated (Table 1). Indeed, we identified the autophosphorylation site (Tyr-416 in human) in the 3 dpf and 5 dpf samples (Table 2, Fig. 3B). This autophosphorylation site is responsible for the regulation of cell adhesion and activity of the kinase. Immunoblot analysis with a phosphospecific antibody recognizing the autophosphorylation site, confirmed the presence of the phosphorylated Src in the lysates and the immunoprecipitates of both samples. Interestingly, the immunoblot showed a significant shift in signal between the 3 and 5 dpf embryo lysates (Fig. 5B). The pSrc 416 antibody cross-reacts with other Src-family kinase members (Fyn or Yes) since this phosphorylation site is conserved throughout the family. The observed shift might indicate a switch in activity from

one member of the family to the other between 3 dpf and 5 dpf embryos. Based on the observed shifts in the immunoblot, Fyn may be present in the lower band and Src or Yes in the higher band. We were able to identify at least one unique peptide for each protein, showing that Src, Fyn and Yes are immunoprecipitated at both stages. Due to the high homology between the three different family members, it was not possible to detect differential expression of the proteins in one of the stages. The role of the Src family kinases in cell signaling is well studied, but less is known about their role in embryonic development. Recent studies underline the importance of tyrosine kinase Fyn and Yes in the early embryonic development of zebrafish (33,34). Our study shows that activity and phosphorylation of the Src family of kinases is still also high at later stages of development and reveals interesting dynamics in expression or post-translational regulation between the 3 and 5 dpf stages.

#### *Eph receptor signaling*

A large family of protein kinases identified in our proteomics assay is the Ephrin receptor (Eph) family of protein-tyrosine kinases. Since Eph receptors and their ephrin ligands are membrane bound, binding and activation requires cell-cell interaction (35). Bidirectional Eph receptor signaling is mainly responsible for the repulsion of neighboring cells or cellular processes, resulting in regulated cell migration, axon guidance and tissue border formation (36,37). Eph receptors are expressed in many tissues during development and receptor activity has been shown to play important roles during development (37-39). The Eph receptor family contains more than 10 members of which we identified about 8 (Table 1) (Due to genome duplication, the zebrafish contains for some Eph receptors an a and b form which are not well annotated yet). For several of these Eph receptors we identified known *in vivo* autophosphorylation sites (Table 2), some of which were also detected in our *in vitro* kinase

assay using the peptide array. We also detected phosphorylation of EphA4, both by MS and reverse IP experiments (Fig 3C, 5E Table 2). Tyrosine phosphorylation of EphA4 has been shown by immunoblotting by Xu *et al.* (40), in earlier stage zebrafish embryo cells. Furthermore, this site has been previously reported by Rush *et al.* (23) (PhosphoSite; www.phosphosite.org). Our data suggest an important role for the various Eph receptors and their tyrosine phosphorylation and activation in the embryonic signaling pathways.

### *Conclusion*

In summary, in this study tyrosine phosphorylation was analyzed using proteomics technologies in whole zebrafish *in vivo* to investigate signaling in zebrafish development at day 3 and 5 post fertilization. Differences in protein expression and in protein phosphorylation were observed, suggesting that notable signaling occurs intended for focal adhesion, cell adhesion, cell sorting in axon guidance and in tissue border formation and also for a number of other processes that are important in late embryogenesis. *In vivo* observed tyrosine phosphorylation could be complemented by detection of *in vitro* kinase activities and confirmed by Western blotting experiments. This shows the value of the complementary use of three technologies in the field of functional proteomics.

## References

1. Salomon, A. R., Ficarro, S. B., Brill, L. M., Brinker, A., Phung, Q. T., Ericson, C., Sauer, K., Brock, A., Horn, D. M., Schultz, P. G., and Peters, E. C. (2003). Profiling of tyrosine phosphorylation pathways in human cells using mass spectrometry. *Proc Natl Acad Sci U S A* 100 2, 443-448
2. Blagoev, B., Kratchmarova, I., Ong, S. E., Nielsen, M., Foster, L. J., and Mann, M. (2003). A proteomics strategy to elucidate functional protein-protein interactions applied to EGF signaling. *Nat Biotechnol* 21 3, 315-318
3. Brill, L. M., Salomon, A. R., Ficarro, S. B., Mukherji, M., Stettler-Gill, M., and Peters, E. C. (2004). Robust phosphoproteomic profiling of tyrosine phosphorylation sites from human T cells using immobilized metal affinity chromatography and tandem mass spectrometry. *Anal Chem* 76 10, 2763-2772
4. Thelemann, A., Petti, F., Griffin, G., Iwata, K., Hunt, T., Settineri, T., Fenyo, D., Gibson, N., and Haley, J. D. (2005). Phosphotyrosine signaling networks in epidermal growth factor receptor overexpressing squamous carcinoma cells. *Mol Cell Proteomics* 4 4, 356-376
5. Blagoev, B., Ong, S. E., Kratchmarova, I., and Mann, M. (2004). Temporal analysis of phosphotyrosine-dependent signaling networks by quantitative proteomics. *Nat Biotechnol* 22 9, 1139-1145
6. Beis, D., and Stainier, D. Y. (2006). In vivo cell biology: following the zebrafish trend. *Trends Cell Biol* 16 2, 105-112
7. Dooley, K., and Zon, L. I. (2000). Zebrafish: a model system for the study of human disease. *Curr Opin Genet Dev* 10 3, 252-256
8. Grunwald, D. J., and Eisen, J. S. (2002). Headwaters of the zebrafish -- emergence of a new model vertebrate. *Nat Rev Genet* 3 9, 717-724
9. Driever, W., Solnica-Krezel, L., Schier, A. F., Neuhauss, S. C., Malicki, J., Stemple, D. L., Stainier, D. Y., Zwartkruis, F., Abdelilah, S., Rangini, Z., Belak, J., and Boggs, C. (1996). A genetic screen for mutations affecting embryogenesis in zebrafish. *Development* 123, 37-46
10. Haffter, P., Granato, M., Brand, M., Mullins, M. C., Hammerschmidt, M., Kane, D. A., Odenthal, J., van Eeden, F. J., Jiang, Y. J., Heisenberg, C. P., Kelsh, R. N., Furutani-Seiki, M., Vogelsang, E., Beuchle, D., Schach, U., Fabian, C., and Nusslein-Volhard, C. (1996). The identification of genes with unique and essential functions in the development of the zebrafish, *Danio rerio*. *Development* 123, 1-36
11. Cooper, J. A., Sefton, B. M., and Hunter, T. (1983). Detection and quantification of phosphotyrosine in proteins. *Methods Enzymol* 99, 387-402
12. Link, V., Shevchenko, A., and Heisenberg, C. P. (2006). Proteomics of early zebrafish embryos. *BMC Dev Biol* 6, 1
13. Westerfield, M. (2000). The zebrafish book. A guide for the laboratory use of the zebrafish (*Danio rerio*). *Eugene, Univ. of Oregon Press* 4th edition
14. Gobom, J., Nordhoff, E., Mirgorodskaya, E., Ekman, R., and Roepstorff, P. (1999). Sample purification and preparation technique based on nano-scale reversed-phase columns for the sensitive analysis of complex peptide mixtures by matrix-assisted laser desorption/ionization mass spectrometry. *J Mass Spectrom* 34 2, 105-116
15. Meiring, H. D., van der Heeft E., ten Hove G.J., and de Jong A.P.J.M. (2002). Nanoscale LC-MS[(n)]: technical design and applications to peptide and protein analysis. *J. Sep. Sci.* 25 9, 557-568

16. Nesvizhskii, A. I., Keller, A., Kolker, E., and Aebersold, R. (2003). A statistical model for identifying proteins by tandem mass spectrometry. *Anal Chem* 75 17, 4646-4658
17. Hokaiwado, N., Asamoto, M., Tsujimura, K., Hirota, T., Ichihara, T., Satoh, T., and Shirai, T. (2004). Rapid analysis of gene expression changes caused by liver carcinogens and chemopreventive agents using a newly developed three-dimensional microarray system. *Cancer Sci* 95 2, 123-130
18. Wu, Y., de Kievit, P., Vahlkamp, L., Pijnenburg, D., Smit, M., Dankers, M., Melchers, D., Stax, M., Boender, P. J., Ingham, C., Bastiaensen, N., de Wijn, R., van Alewijk, D., van Damme, H., Raap, A. K., Chan, A. B., and van Beuningen, R. (2004). Quantitative assessment of a novel flow-through porous microarray for the rapid analysis of gene expression profiles. *Nucleic Acids Res* 32 15, e123
19. van Beuningen, R., van Damme, H., Boender, P., Bastiaensen, N., Chan, A., and Kievits, T. (2001). Fast and specific hybridization using flow-through microarrays on porous metal oxide. *Clinical Chemistry* 47, 1931-1933
20. Lemeer, S., Jopling, C., Naji, F., Ruijtenbeek, R., Slijper, M., Heck, A. J., and den Hertog, J. (2007). Protein-tyrosine kinase activity profiling in knock down zebrafish embryos. *PLoS ONE* 2, e581
21. Beausoleil, S. A., Jedrychowski, M., Schwartz, D., Elias, J. E., Villen, J., Li, J., Cohn, M. A., Cantley, L. C., and Gygi, S. P. (2004). Large-scale characterization of HeLa cell nuclear phosphoproteins. *Proc Natl Acad Sci U S A* 101 33, 12130-12135
22. Amanchy, R., Kalume, D. E., Iwahori, A., Zhong, J., and Pandey, A. (2005). Phosphoproteome analysis of HeLa cells using stable isotope labeling with amino acids in cell culture (SILAC). *J Proteome Res* 4 5, 1661-1671
23. Rush, J., Moritz, A., Lee, K. A., Guo, A., Goss, V. L., Spek, E. J., Zhang, H., Zha, X. M., Polakiewicz, R. D., and Comb, M. J. (2005). Immunoaffinity profiling of tyrosine phosphorylation in cancer cells. *Nat Biotechnol* 23 1, 94-101
24. Mukherji, M., Brill, L. M., Ficarro, S. B., Hampton, G. M., and Schultz, P. G. (2006). A Phosphoproteomic Analysis of the ErbB2 Receptor Tyrosine Kinase Signaling Pathways. *Biochemistry* 45 51, 15529-15540
25. Zhang, Y., Wolf-Yadlin, A., Ross, P. L., Pappin, D. J., Rush, J., Lauffenburger, D. A., and White, F. M. (2005). Time-resolved mass spectrometry of tyrosine phosphorylation sites in the epidermal growth factor receptor signaling network reveals dynamic modules. *Mol Cell Proteomics* 4 9, 1240-1250
26. Tay, T. L., Lin, Q., Seow, T. K., Tan, K. H., Hew, C. L., and Gong, Z. (2006). Proteomic analysis of protein profiles during early development of the zebrafish, *Danio rerio*. *Proteomics* 6 10, 3176-3188
27. Hagel, M., George, E. L., Kim, A., Tamimi, R., Opitz, S. L., Turner, C. E., Imamoto, A., and Thomas, S. M. (2002). The adaptor protein paxillin is essential for normal development in the mouse and is a critical transducer of fibronectin signaling. *Mol Cell Biol* 22 3, 901-915
28. Schaller, M. D., and Parsons, J. T. (1995). pp125FAK-dependent tyrosine phosphorylation of paxillin creates a high-affinity binding site for Crk. *Mol Cell Biol* 15 5, 2635-2645
29. Crawford, B. D., Henry, C. A., Clason, T. A., Becker, A. L., and Hille, M. B. (2003). Activity and distribution of paxillin, focal adhesion kinase, and cadherin indicate cooperative roles during zebrafish morphogenesis. *Mol Biol Cell* 14 8, 3065-3081
30. Turner, C. E. (1991). Paxillin is a major phosphotyrosine-containing protein during embryonic development. *J Cell Biol* 115 1, 201-207



31. Schaller, M. D., and Schaefer, E. M. (2001). Multiple stimuli induce tyrosine phosphorylation of the Crk-binding sites of paxillin. *Biochem J* 360 Pt 1, 57-66
32. Hsia, D. A., Mitra, S. K., Hauck, C. R., Streblov, D. N., Nelson, J. A., Ilic, D., Huang, S., Li, E., Nemerow, G. R., Leng, J., Spencer, K. S., Cheresch, D. A., and Schlaepfer, D. D. (2003). Differential regulation of cell motility and invasion by FAK. *J Cell Biol* 160 5, 753-767
33. Jopling, C., and den Hertog, J. (2005). Fyn/Yes and non-canonical Wnt signalling converge on RhoA in vertebrate gastrulation cell movements. *EMBO Rep* 6 5, 426-431
34. Tsai, W. B., Zhang, X., Sharma, D., Wu, W., and Kinsey, W. H. (2005). Role of Yes kinase during early zebrafish development. *Dev Biol* 277 1, 129-141
35. Davis, S., Gale, N. W., Aldrich, T. H., Maisonpierre, P. C., Lhotak, V., Pawson, T., Goldfarb, M., and Yancopoulos, G. D. (1994). Ligands for EPH-related receptor tyrosine kinases that require membrane attachment or clustering for activity. *Science* 266 5186, 816-819
36. Klein, R. (1999). Bidirectional signals establish boundaries. *Curr Biol* 9 18, R691-694
37. Mellitzer, G., Xu, Q., and Wilkinson, D. G. (1999). Eph receptors and ephrins restrict cell intermingling and communication. *Nature* 400 6739, 77-81
38. Cooke, J. E., Kemp, H. A., and Moens, C. B. (2005). EphA4 is required for cell adhesion and rhombomere-boundary formation in the zebrafish. *Curr Biol* 15 6, 536-542
39. Mellitzer, G., Xu, Q., and Wilkinson, D. G. (2000). Control of cell behaviour by signalling through Eph receptors and ephrins. *Curr Opin Neurobiol* 10 3, 400-408
40. Xu, Q., Mellitzer, G., Robinson, V., and Wilkinson, D. G. (1999). In vivo cell sorting in complementary segmental domains mediated by Eph receptors and ephrins. *Nature* 399 6733, 267-271

## Acknowledgements

The authors wish to thank David Wilkinson for the anti-EphA4 antibody. The authors are grateful to dr. Bas van Breukelen for his kind support with the BLAST searches. EU research training network HPRN-CT-2000-00085, NWO (grant no. 015.001.131) and the Netherlands Proteomics Centre supported this research ([www.netherlandsproteomicscentre.nl](http://www.netherlandsproteomicscentre.nl)).

**Supporting information available:** All MS/MS spectra are available as a Scaffold-file at [https://bioinformatics.chem.uu.nl/supplementary/lemeer\\_mcp](https://bioinformatics.chem.uu.nl/supplementary/lemeer_mcp). This file includes protein and peptide scoring and information on PTMs. The Scaffold viewer is also available for download.

## Abbreviations

BLAST	-	basic logical alignment and research tool
DPF	-	days post fertilization
HNTG-buffer	-	buffer containing Hepes, NaCl, Triton X-100, and glycerol
ID	-	Inner diameter
IP	-	immunoprecipitation
IPI	-	international protein index
LTQ-FT-ICR	-	linear ion trap coupled to Fourier-transform ion cyclotron resonance mass spectrometer
LC	-	Liquid chromatography
MS	-	Mass spectrometry
MS <sup>2</sup>	-	Tandem MS or MS/MS
MS <sup>3</sup>	-	Neutral loss dependent MS/MS/MS
NCBI-nr	-	National Center for Biotechnology Information non-redundant
RP	-	Reversed phase
RT	-	Room temperature
PTK	-	protein tyrosine kinases
PTP	-	protein tyrosine phosphatases
pTyr	-	phosphorylated tyrosine residue
SCX	-	strong cation exchange chromatography
TCA	-	Tricarboxylic acid

## Figure legends

**Fig. 1. Experimental scheme for the analysis of endogenous *in vivo* tyrosine phosphorylation during zebrafish development.** **A** Lateral view of 3 dpf (left) and 5 dpf (right) zebrafish embryo. **B.** The lysates from 3 dpf and 5 dpf embryos were used for direct *in vitro* kinase assays on a peptide micro-array chip. Alternatively, tyrosine phosphorylated proteins were immunoprecipitated by anti-pTyr antibodies and immunoprecipitated proteins were eluted from the antibodies using phenylphosphate. A small portion (1/25) of the eluted proteins was subjected to SDS-PAGE and immunoblotted with 5 different antibodies. The majority of eluted proteins were digested, and the resulting peptides were separated first by strong cation exchange (SCX) and subsequently (each of the obtained SCX fractions) further by nanoRP chromatography. Peptides were analyzed and identified by MS<sup>2</sup> and MS<sup>3</sup> using a LTQ-FT-ICR mass spectrometer.

**Fig. 2. Enrichment of tyrosine phosphorylated proteins from 3 dpf and 5 dpf zebrafish embryos.**

Anti pTyr immunoblot showing enrichment of tyrosine phosphorylated proteins from 3 and 5 dpf embryo lysates, using anti-pTyr immunoprecipitation. The 3 dpf embryos were deyolked prior to lysis. Lysates (corresponding to 5 embryo equivalents) and immunoprecipitates (corresponding to 75 embryo equivalents) were separated via SDS-PAGE and blotted and probed with PY20. Detection was done using enhanced chemiluminescence and is depicted here. After specific elution, a clear enrichment of phosphorylated proteins is observed in the immunoprecipitates (IP). The boiled immunoaffinity beads do not give any significant signal (only light and heavy chains of the antibody), indicating that specific elution using phenylphosphate was very efficient (Beads).

**Fig. 3. MS<sup>2</sup> spectra from identified phosphopeptides**

A. MS<sup>2</sup> spectrum of QGVFLPEETpYSCPR from Paxillin; B. MS<sup>2</sup> spectrum of LIEDNEpYTAR from the Src Family of Kinases (SFK); C. MS<sup>2</sup> spectrum of VLEDDPEAApYTTR from Eph receptor EphA4b; D. MS<sup>2</sup> spectrum of LTDDMTGpYVATR from Mitogen-activated protein kinase 14b.

#### **Fig. 4. *In vitro* kinase assays are consistent with *in vivo* phosphorylation**

Kinase assays were performed using lysates of 3 dpf and 5 dpf zebrafish embryos, with arrays of 144 peptides encoding known tyrosine phosphorylation sites. Kinase reaction and detection is described in materials and methods section. Pictures of the endpoints of the kinase reactions from 5 dpf (A), 3 dpf (B) and 5 dpf in the absence of ATP (C) are shown here. D. Selection of peptides that were present on the chip. Numbers refer to position of the peptides on the chip in A and B. The identity of the proteins, the phosphopeptides detected by MS and the sequence of the peptides on the chip are indicated. (E) Correlation graph between spot intensities after incubation with 5 dpf (x-axis) and 3 dpf (y-axis) embryo lysates. The panel on the right is an enlargement of the low intensity region left.

#### **Fig. 5 Validation of tyrosine phosphorylation of selected proteins by immunoblotting.**

Zebrafish embryos were lysed at 3 or 5 dpf and immunoprecipitated with anti-pTyr antibodies (5 A,B,C,D). Immunoprecipitated proteins were specifically eluted with phenylphosphate. Lysates (corresponding to 5 embryo equivalents) and immunoprecipitates (corresponding to 75 embryo equivalents) were loaded on SDS-PAGE and blotted. Blots were probed with the indicated antibodies. A. Paxillin; B. pSrc418; C. EphA4; D. Actin. For reverse immunoprecipitations (5 E,F), 3 and 5 dpf zebrafish embryos were lysed and immunoprecipitation was performed with anti-paxillin (5E) or anti-EphA4 (5F) antibody. Immunoprecipitates (corresponding to 75 embryo equivalents) were loaded on SDS-PAGE and blotted. Blots were probed with the corresponding antibody, anti-paxillin (5E) or EphA4 (5F) to detect immunoprecipitation of the protein of interest. Subsequently, blots were stripped and probed with anti-phosphotyrosine antibody. Detection was performed by enhanced chemiluminescence.

## Table legends

### **Table 1. Identified phosphotyrosine signaling proteins in 3 and 5 dpf zebrafish embryos.**

Proteins from 3 and 5 dpf zebrafish embryos that (co-)immunoprecipitated with anti-phosphotyrosine antibodies were identified with LC-FT-ICR-MS<sup>n</sup>. These selected proteins are discussed in the text. A list of all identified proteins is given in the Supplementary Table 1. The potential function of the protein was established by BLAST homology searches. The sequence coverage and cumulative number of detected unique peptides from three independent experiments are listed, both for the 3 and 5 dpf samples. Identified proteins confirmed by immunoblotting are indicated in bold. More details can be found in the Materials and Methods section and in the supplementary Scaffold-file [https://bioinformatics.chem.uu.nl/supplementary/lemeer\\_mcp](https://bioinformatics.chem.uu.nl/supplementary/lemeer_mcp).

### **Table 2. Identified *in vivo* phosphorylation sites**

Phosphopeptides were identified using LC-LTQ-FT-ICR-MS<sup>2</sup> and LC-LTQ-FT-ICR-MS<sup>3</sup> analysis. Some typical examples of these spectra are given in Fig. 3.

### **Supplementary Table 1. Protein identifications from the anti-phosphotyrosine immunoprecipitations.**

Proteins identified with 2D LC-LTQ-FT-ICR-MS<sup>n</sup> in 3 dpf and 5 dpf embryos after enrichment through phosphotyrosine immunoprecipitation. Proteins were identified using the IPI zebrafish database (version 3.16). The number of cumulative unique peptides detected for each stage from three independent experiments is indicated.

### **Supplementary Table 2. Peptide sequences on PamChip**

Protein name and amino acid sequences from peptides immobilized on the chip and the corresponding phosphorylation site, derived from Swissprot and/or Phosphobase database. The position on the chip is indicated, characters representing rows, numbers representing columns.

### **Supplementary Spectra 1**

MS<sup>2</sup> and MS<sup>3</sup> spectra from phosphopeptides identified in 3dpf immunoprecipitates

### **Supplementary Spectra 2**

MS<sup>2</sup> and MS<sup>3</sup> spectra from phosphopeptides identified in 5dpf immunoprecipitates

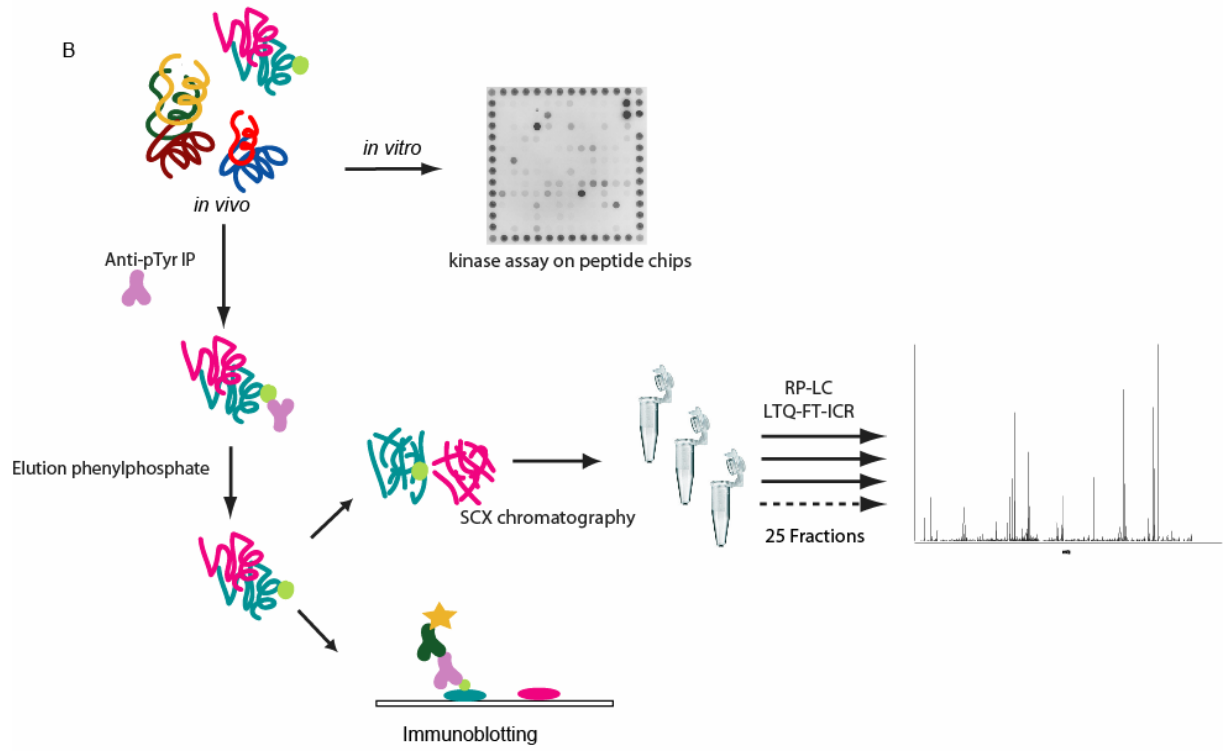
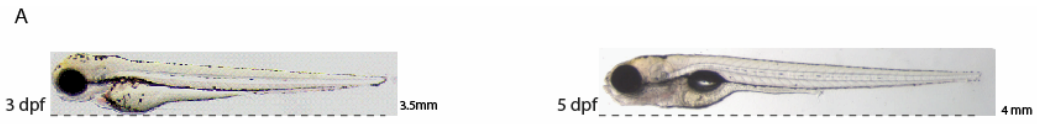


**Figure 1.**

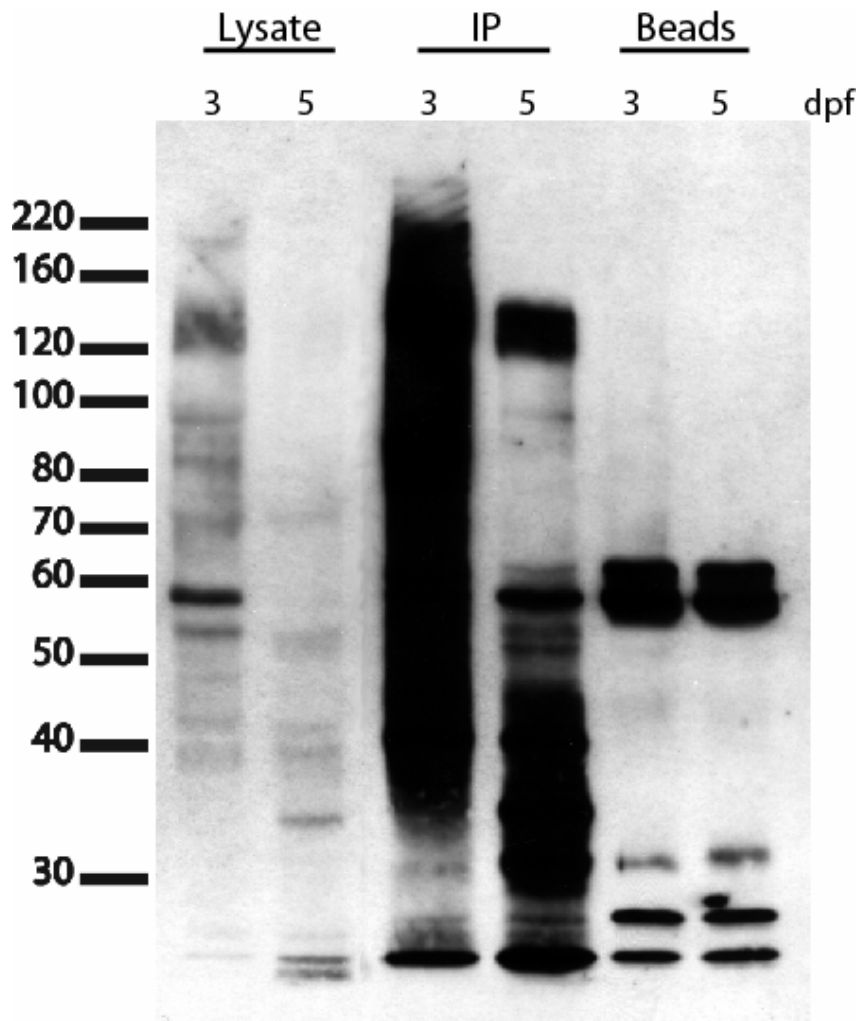


Figure 2.



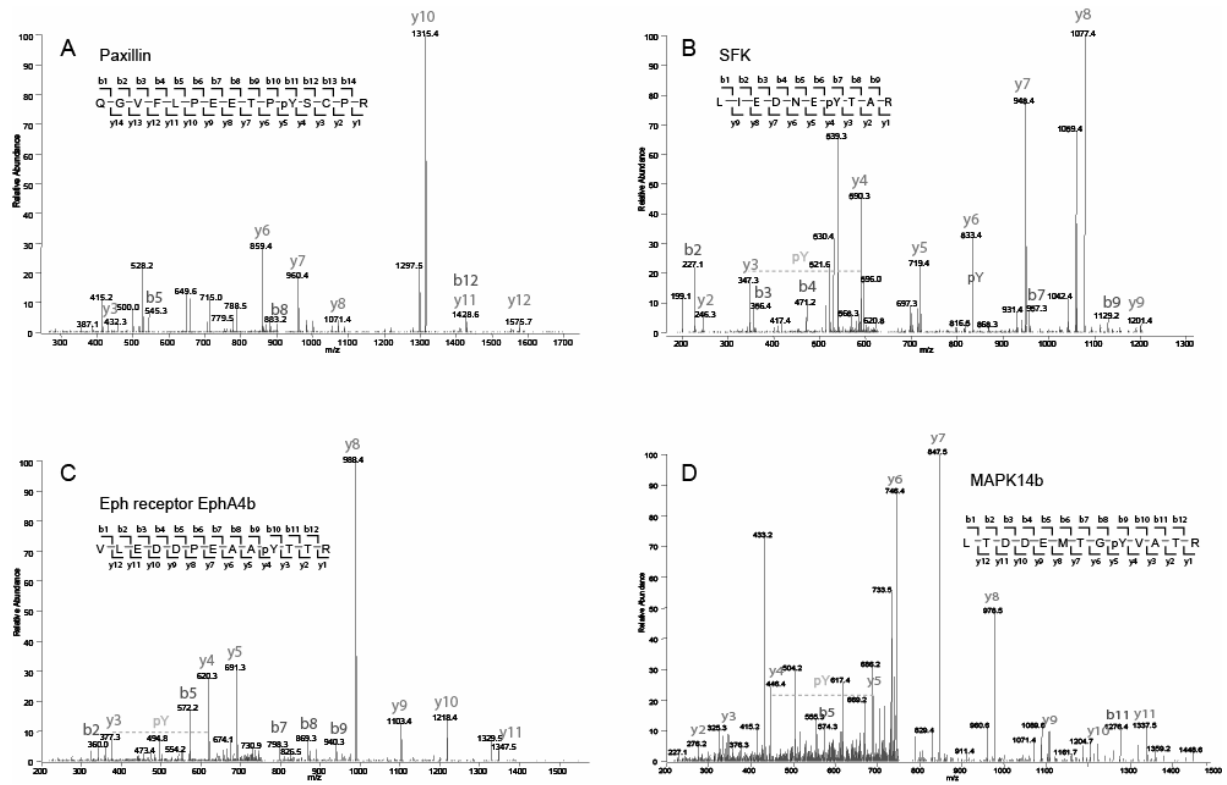


Figure 3.

Figure 4 Lemeer et al.

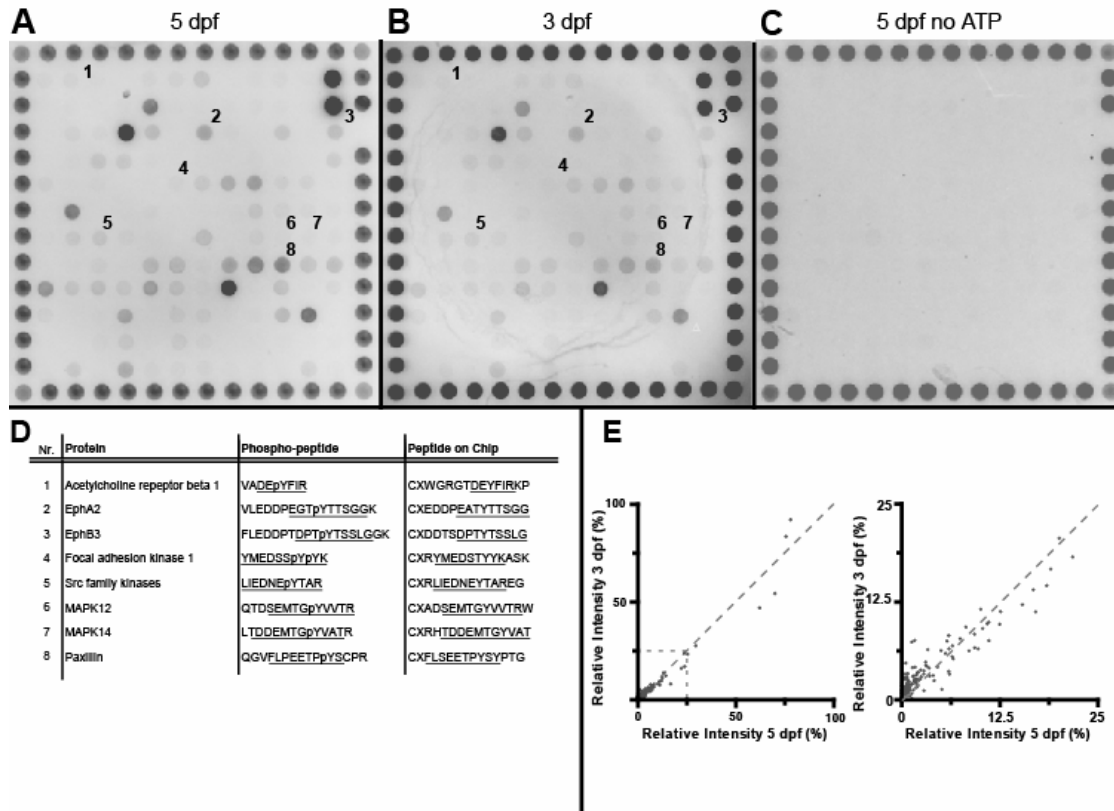


Figure 4.

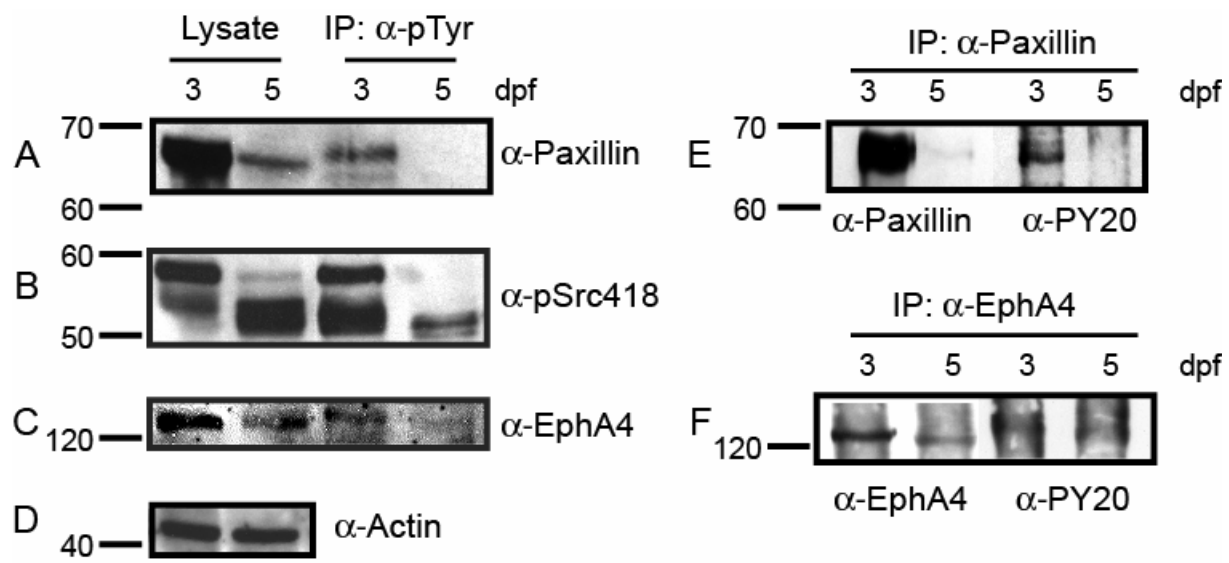


Figure 5.